

Degradation behaviour of a composite material for thermal protection systems

Part I—Experimental characterization

L. TORRE, J. M. KENNY

Institute of Chemical Technology, University of Perugia, Loc. Pentima bassa, 05100, Terni, Italy
E-mail: torrel@unipg.it

A. M. MAFFEZZOLI

Department of Materials Science, University of Lecce, Via per Arnesano, 73100, Lecce, Italy

Thermogravimetric studies and combined thermal analysis techniques have been used to characterize an ablative composite for thermal protection systems. The aim of the work was to utilize these techniques to obtain the main parameters used in the computer simulation of the space re-entry. In particular, a phenomenological model of the degradation kinetics of a silicon-based ablative composite has been developed using thermogravimetric analysis coupled with mass spectroscopic analysis. Simultaneous thermal analysis has also been used to calculate the ablation heat. The results are used as input for a computer model, developed in Part II, to enable calculation of the temperature profiles inside a thermal protection shield during the re-entry into the earth's atmosphere. Such a program can also be used in materials selection. © 1998 Kluwer Academic Publishers

1. Introduction

The degradative processes of polymer composites are commonly considered as phenomena that lead to the disruption of a part and therefore to be avoided. Thus, degradation studies are usually intended to provide a database for industrial practices, in order to ascertain the processing parameters and the working conditions that could prevent the degradation of the material. However, there are other cases in which a material is used for its capacity to degrade, in this case the degradation ability is responsible for the good performance of the material. Ablative materials, used for active thermal shields during re-entry of space vehicles [1], are a classical example of such materials. In order to protect the space vehicle from the huge amount of heat produced by the friction of the atmosphere, ablative materials degrade through endothermic reactions, absorbing the heat and avoiding its transfer to the interior of the vehicle. The main phenomena occurring in the ablation process are heat transfer, chemical reactions and fluid flow.

1.1. The ablation process

Ablation is an effective and reliable method largely used in aerospace structures to protect the payload from the damaging effects of external high temperatures. In the ablation process, the high heat fluxes are dissipated by the material through a series of

endothermic processes, that finally lead to the loss and the consumption of the material itself. The working process of an ablative heat shield can be briefly summarized as follows. The convective heat that reaches the vehicle surface is balanced by surface radiation, phase transitions (melting, vaporization), and/or chemical reactions (charring degradation). Moreover, part of the incoming convective heat flux is blocked by the outcoming flow of hot gases that result from the degradative processes (ablative blockage and blowing). The ablative material keeps the surface temperature within a certain range, and as a consequence an increase of the heat flux will not cause a consistent temperature rise, but will cause an increase of the surface "recession rate". Therefore, important parameters in the choice of a suitable ablator, are the ablation temperature (the temperature at which the material degradation begins) and the density [2, 3].

The most significant properties of an ablative material are specific heat, thermal conductivity and density. In particular, the density is characterized by a lower limit dictated by the necessity of a low recession rate, and an upper limit dictated by the lightweight requirements of all the aerospace parts. Furthermore, the degradation of an ablative material has to be an endothermic reaction, yielding a fair amount of gases.

Such different properties are barely attained by a single material, therefore, most commercial ablators

are composite materials. As in the case of traditional composites, ablative materials have matrix and fillers, each of them contributing to different properties. Several different fillers can be used. For example, in order to satisfy the weight reduction requirement, a low density filler (hollow spheres) can be used, while to contribute to the formation of a porous char skeleton where the gases can flow through as the degradation reaction evolves, a reactive filler, together with a small amount of fibrous reinforcements, can be used [2]. In general, the degradation reaction affects mainly the matrix. In fact, most of the matrices of ablative materials are made out of polymers, taking advantage of the highly endothermic nature of polymer degradation in non-oxidative atmospheres, and of their many good properties such as low density, low thermal conductivity, high specific heat, in addition to excellent mechanical properties.

In summary, the polymeric constituent in an ablator basically has to accomplish two functions. First it degrades thereby absorbing energy, and second it serves as a binder for the other components. The most commonly used resins are phenol formaldehyde, epoxies, silicones, and polytetrafluoroethylene [2, 4, 5]. Fillers used for ablative materials include carbon fibres, silica fibres, and other low-density fillers. Low-density fillers include phenolic micro-balloons, glass-microspheres, silica macrospheres, and cork [4, 6, 7].

1.2. Charring ablative materials

Charring ablators produce char as an effect of the degradation reaction, subsequently providing an insulation layer. During the ablation reaction, these materials do not reduce their volume significantly. Moreover, charring ablators are the most widely used thermal protection shields and are generally produced with phenolic, epoxy, or silicon resins reinforced with glass, silica or organic spheres and short fibres [8–10]. As the charring ablator is heated, the temperature increases until the surface reaches the degradation temperature and starts to release gaseous products, leaving a porous, carbonaceous residue (char). The pyrolysis temperature, ranging from 250–600 °C, is relatively low, and it is a function of the local pressure and the heating rate. As the shield continues to heat up, the pyrolysis zone proceeds into the material and the decomposition occurs below the surface. The gaseous products diffuse through the porous char to the surface and, during this stage, they absorb energy from the char and continue to react undergoing further decomposition. Finally, the exhausted gases exit into the boundary layer where they provide a further barrier for the heat exchange, and may undergo additional chemical reaction with the boundary layer gas.

The char is primarily carbonaceous and continues to absorb heat until it reaches the temperature at which it oxidizes, or sublimates, or is mechanically removed by external shear forces. For lifting or moderate ballistic re-entry, oxidation is the main thermochemical char-removal mechanism [2]. At surface temperatures below 800 °C, oxidation is limited by reaction rate kinetics. In this regime, surface recession

can be reduced appreciably by incorporating oxidation-resistant additives such as silica. As the surface temperature increases, the oxidation rate increases exponentially until the oxygen at the surface begins to be depleted. At still higher temperatures the surface recession is limited by the rate at which the oxygen can diffuse through the boundary layer. In this regime the mass rate of char oxidation is virtually independent of material properties. At a temperature of about 3000 °C, the char sublimates.

However, the char formed by a homogeneous plastic is usually weak and brittle, making the material susceptible to rapid removal by mechanical shear and spallation (coming from thermal stresses and internal pressure build-up). This fact reduces the insulation efficiency of the char, and exposes the cooler internal material to the surface conditions, resulting in a less radiative cooling process. To improve the char retention characteristics of the ablative resins, reinforcing fibres are commonly added to these materials. Furthermore, a fundamental role of the char is to block oxygen diffusion from the boundary layer to the virgin material. In fact the requested endothermic degradation reactions of the polymeric matrix occurs only in a non-oxidative atmosphere. A fast recession rate of the protective char material could result in an undesired exothermic oxidative process.

The scope of this work was to define a characterization procedure for the performances of an ablative material and of the ablation process. In particular, the work focused on how thermal analysis techniques can be applied in order to obtain information on the behaviour of ablative materials. The use of thermal analysis will be finalized to obtain the input parameters for a model of a simple ablation process in a thermal shield described in Part II [11]. Thermogravimetric analysis will be used to evaluate and study the rate of decomposition kinetics of a complex model ablative system formed by silicon resin and reinforced with phenolic and quartz spheres [12]. Differential scanning calorimetry (DSC) and combined techniques (STA) will also be used to evaluate the ablation heat.

2. Experimental procedure

An ablative material, kindly provided by Alenia Spazio S.p.A., was used in this study. The components and a general indication of their relative amount are reported in Table I.

Different thermal analysis techniques have been used to evaluate the performance of the ablative material. A thermogravimetric analyser (TG), TA Instrument 9100, has been used to study the degradation kinetics in non-isothermal conditions. Moreover, differential scanning analysis (DSC) has been used to calculate the heat of ablation. In particular, in order to take into account both heat fluxes and weight losses, simultaneous thermal analysis (STA) DSC-TG, Netzsch 498, has been used. The calorimetric sensitivity curve of the DSC cell was determined using seven different pure metals. Thermal analysis experiments have been performed in a nitrogen atmosphere ($200 \text{ cm}^3 \text{ min}^{-1}$), simulating the non-oxidative

TABLE I Components of the ablative material used

Component	Amount (%)
Poly (methyl phenyl siloxane) filled with Fe ₂ O ₃	50%
Hollow phenolic microspheres	22%
Quartz microfibrres	Not available
Hollow silica microspheres	Not available

conditions occurring at the surface of the ablator. An STA experiment was conducted in the presence of an air flow for comparison purposes. In order to better investigate the degradation mechanism, a Balzers mass spectrometer has been coupled with the STA system.

3. Analysis of the performances of ablative materials

3.1. Enthalpy of pyrolysis gases

Simultaneous thermal analysis provides a direct measurement of the heat of ablation by integration of the reaction peak corrected by the weight loss contribution. An STA test on the material in nitrogen, gives a broad endothermic peak from 250 and 700 °C, in order to obtain exact values of the heat of ablation, some modification should be made. Fig. 1 is, in fact, obtained by modifying the output signal, S , taking into account the actual weight of the sample, m , and the calorimetric sensitivity of the DSC cell, $C(T)$ according to

$$\frac{dQ}{dt} = \frac{S}{C(T)m} \quad (1)$$

The heat absorbed during the ablation process, namely Q , corresponding to the area under the heat flow curve in Fig. 2, can be obtained by integration of the peak with respect of the baseline indicated in the figure, namely

$$Q = \int_{t_1}^{t_2} \left(\frac{dQ}{dt} - BL \right) dt \quad (2)$$

where BL is the linear baseline temperature function. The heat of ablation calculated by integration of the peak in Fig. 2 is 2256 J g⁻¹. Fig. 2 also gives the STA result obtained in an air atmosphere. From this picture is possible to observe that the ablative behaviour is manifested only in a non-oxidative atmosphere, an exothermic peak of 3542 J g⁻¹ was, in fact, obtained in this case.

3.2. Degradation kinetics by TGA

TGA experiments have been performed both in dynamic and in isothermal mode, in order to obtain the variation of the sample weight as a function of time and temperature required to model the ablation reaction kinetics. Furthermore, in order to better understand the reaction mechanism, an elementary analysis of the evolved gases has been performed using a mass spectrometer.

As mentioned above, the phenomena that occur during ablative degradation are complicated by the nature of the material that is a mixture of different

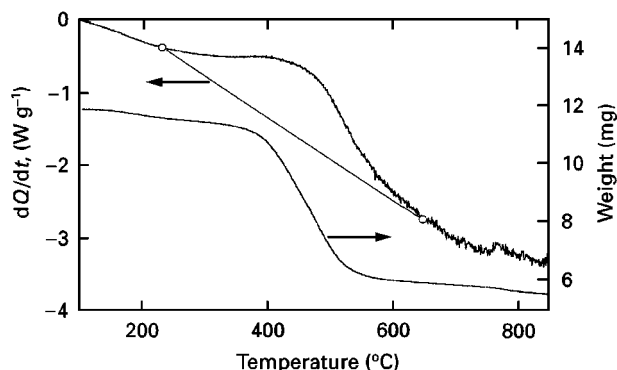


Figure 1 Simultaneous thermal analysis run in nitrogen on the ablative material, with the baseline correction. Heat of degradation = 2256 J g⁻¹.

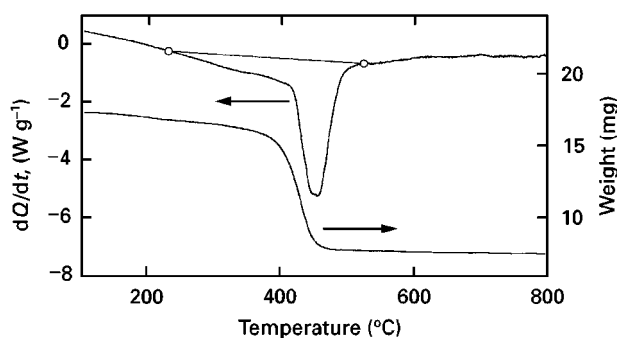


Figure 2 Simultaneous thermal analysis run in air on the ablative material. Heat of degradation = - 3542 J g⁻¹.

components. In the specific case of the material analysed in this research, both the matrix (silicone resin) and one of the fillers (phenolic microspheres) can both participate in the degradation reaction. Experimental evidence is therefore needed to establish if the degradation processes of the two components present in the ablative material are independent. In order to verify whether the two reactions are independent, the following tests were performed. TGA dynamic tests from room temperature to the temperature at which the reaction is completed (almost 1000 °C), performed on samples of pure phenolic microspheres and pure silicone resin, are reported in Fig. 3. Assuming that the two reactions are independent, the following equation should hold

$$W = W_m x_m + W_f x_f \quad (3)$$

where W , W_m and W_f are the individual residual weight fractions of the composite, the silicon resin and the phenolic filler, respectively, and x_m and x_f are the original weight fraction of the matrix and the filler in the composite. If this equation is verified, the determination of the overall reaction rate can be treated as the sum of two independent contributions and so become more simplified. In Fig. 4 the theoretical curve obtained by using Equation 3 is compared with the experimental curve for a dynamic TGA test at 10 °C min⁻¹. From this figure it is evident that the two degradation mechanisms are not independent. Therefore, the determination of the rate of decomposition cannot be split into two problems and a

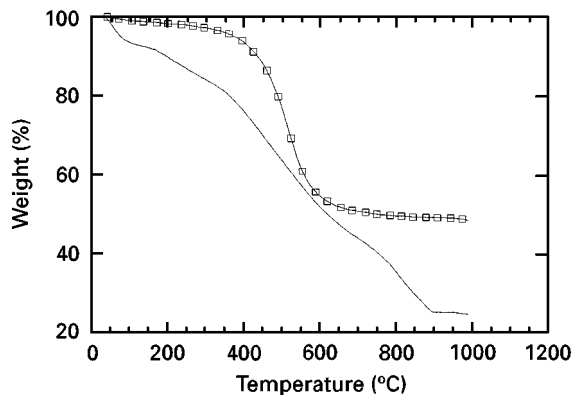


Figure 3 TGA test at $10^{\circ}\text{C min}^{-1}$ for (\square) the silicone and (—) the phenolic resin separately.

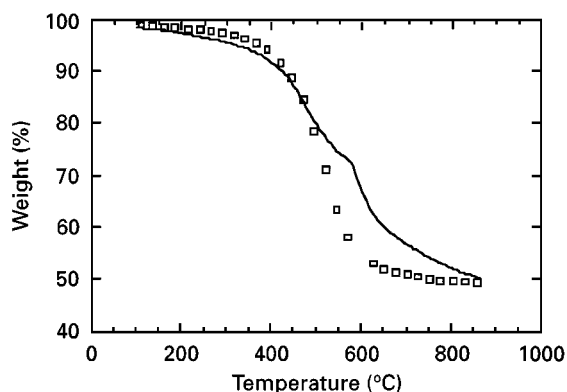


Figure 4 Comparison of (—) the results of Equation 3 and (\square) the experimental data for a TGA test at $10^{\circ}\text{C min}^{-1}$.

phenomenological model that will describe the overall process has to be determined.

Two typical TGA thermograms obtained at different heating rates are reported in Fig. 5. The curve obtained at $5^{\circ}\text{C min}^{-1}$ indicates that at least two different kinetic mechanisms occur. Nevertheless when a slower heating rate is applied, a third kinetic process may be detected above 600°C . The maximum obtainable weight loss is almost the same at heating rates higher than $2^{\circ}\text{C min}^{-1}$. A sensibly lower value of the final weight loss is instead obtained when the test at $1^{\circ}\text{C min}^{-1}$ is performed, as shown in Table II where the results of the experiments are reported. The derivative of the weight loss, reported in Fig. 6, indicated more than one mechanism, as was expected as a consequence of the presence of the two different materials that participate in the degradation process. The first degradation mechanism, probably dominated by the degradation of the phenolic resins, produces about 30% of the weight loss. In order to obtain further insight into the degradation mechanism [13–17], some mass spectrometry tests were performed.

The results obtained at a heating rate of $1^{\circ}\text{C min}^{-1}$ were chosen in order to analyse all the possible degradation mechanisms. The evolved gases were analysed as a function of the temperature. The masses of 18, 44, 28 corresponding, respectively, to H_2O , CO_2 , and CO , gave the stronger signal, while only weak current intensity was measured corresponding to higher mo-

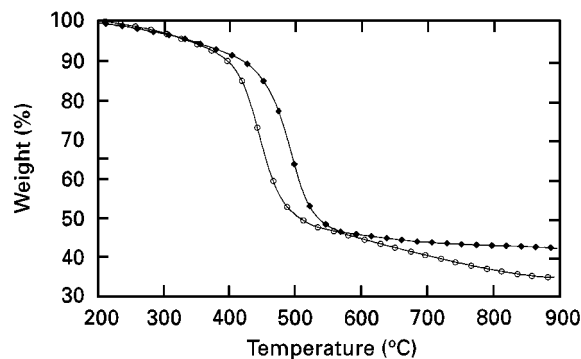


Figure 5 TGA test on the ablative material at two different heating rates: (\circ) $1^{\circ}\text{C min}^{-1}$, (\blacklozenge) $5^{\circ}\text{C min}^{-1}$.

TABLE II Experimental results of the degradation

Heating rate ($^{\circ}\text{C min}^{-1}$)	Temperature range ($^{\circ}\text{C}$)	Weight loss (%)
1	350–900	65
2	360–700	55
5	365–700	57
8	370–700	58
10	372–700	57

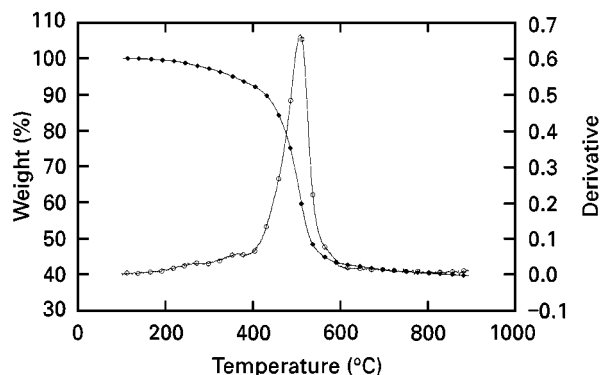


Figure 6 TGA test and derivative of the weight for a dynamic run at $8^{\circ}\text{C min}^{-1}$: (\blacklozenge) weight per cent, (\circ) derivative.

lecular weight species (masses 106–108), and for methyl groups (mass 14–16), the results of the analysis were interpreted in terms of tracking the evolution of H_2O , CO_2 , and CO . The results of these tests are given in Fig. 7. It must be observed that the lower temperature process involves mainly dehydrogenation, while a second process occurring at higher temperature, about 550°C , produces both H_2O and CO_2 . As the temperature increases, the production of carbon dioxide reaches a maximum and then decreases, corresponding to an increase of the CO . This result indicates that the oxidation of carbon occurs in the highest temperature range. It must be pointed out that this last mechanism was not detected at heating rates higher than $2^{\circ}\text{C min}^{-1}$. Another confirmation of this phenomenon came from the visual analysis of the obtained char. In fact, the char obtained at the slow heating rate was white, indicating the absence of carbon in the residual material, while the char obtained at higher heating rates was mainly black.

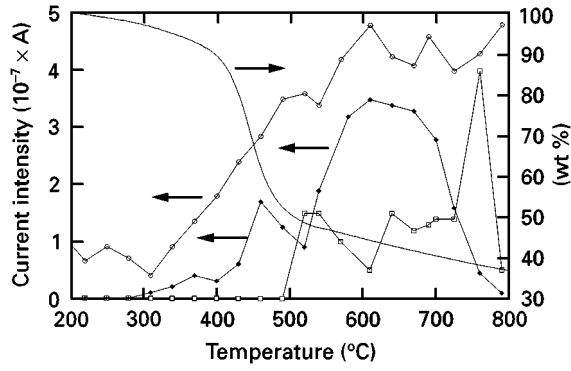
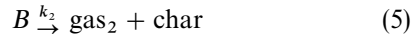
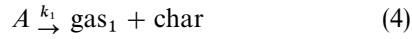


Figure 7 Evolution of (◆) CO₂ (mass 44), (○) H₂O (mass 18) and (□) CO (mass 28) during a dynamic heating at 1 °C min⁻¹.

From the information collected at this point, the degradation of this material appeared to be a process governed mainly by a three-step reaction of which the last one, involving the oxidation of the residual carbon, was observed only at very slow heating rates not commonly encountered during the ablative process. Therefore, a phenomenological model, involving a double degradation process is proposed



The species indicated by A and B are engineering approximations of the reactants in the two-step reaction attributed mainly to the phenolic-controlled reaction and to the silicone-controlled reaction. A model that could consider both processes described in Equations 4 and 5 is therefore a parallel double model proposed also for other materials [18]. The overall degree of degradation, α , is defined as

$$\alpha = \frac{W_0 - W}{W_0 - W_f} \quad (6)$$

where W , W_0 , and W_f are the actual, initial, and final weight of the sample, respectively. The value of W_f was taken as the average value of the residual weights reported in Table II corresponding to 43%. In a parallel kinetic model, α is given by

$$\alpha = y\alpha_1 + (1 - y)\alpha_2 \quad (7)$$

where α_1 and α_2 refer to the degrees of reaction of the processes represented by Equations 4 and 5, respectively. The weight factor, y , taken independent of the temperature, was set equal to 0.3 in accordance with considerations previously reported regarding the form of the derivative curves.

An expression for the rate of reaction is obtained by the time derivative of Equation 8

$$\frac{\partial \alpha}{\partial t} = y \frac{\partial \alpha_1}{\partial t} + (1 - y) \frac{\partial \alpha_2}{\partial t} \quad (8)$$

Finally, each degradation process was represented by a simple n th order kinetic expression

$$\frac{\partial \alpha_i}{\partial t} = K_{0i} \exp\left(-\frac{E_i}{RT}\right) (1 - \alpha_i)^{n_i} \quad i = 1, 2 \quad (9)$$

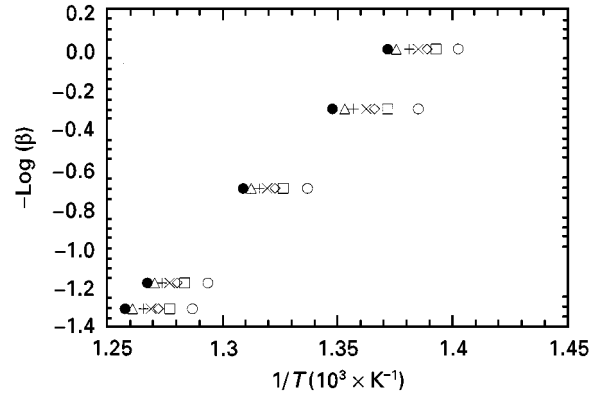


Figure 8 Flynn-Wall isoconversion plot for the whole range of degrees of reaction of the degradation: (○) 0.40, (□) 0.45, (◇) 0.47, (×) 0.49, (+) 0.51, (△) 0.53, (●) 0.55.

In order to determine the parameters of Equation 9, a non-linear kinetic analysis is used. Because the two reaction mechanisms previously mentioned were shown to be a strong function of temperature and heating rate, the activation energy and the pre-exponential factor cannot be calculated from isothermal tests, because the isotherms would not reflect the real reaction mechanism. Therefore, dynamic tests were used for the kinetic analysis.

Several methods presented in the literature, use the possibility of calculating the kinetic parameters, without using the isothermal tests [19–21]. In particular the Flynn and Wall method was used in this study to determine a value of the activation energy for each of the two mechanisms, that could be later used as a first tentative value in the non-linear regression analysis. The Flynn and Wall method allows the determination of the activation energy from dynamic tests by plotting the logarithm of heating rate, β , as a function of the inverse of the temperature, at different conversions. At each fixed conversion a number of points equal to the number of the dynamic tests performed will be obtained; if these points lie on parallel lines for all the conversion, the slope of this plot will give the value of the activation energy, E

$$\frac{\partial \log(\beta)}{\partial (T^{-1})} \cong \left(\frac{0.457}{R}\right) E \quad (10)$$

The Flynn and Wall method was then applied to study the behaviour of the activation energy of the decomposition and therefore to obtain a starting value for the analysis of the parameters of Equation 9. Fig. 8 shows an isoconversion plot for the degradation at nine different degrees of conversion. At slow heating rates and high degree of conversion (upper left corner of the plot), a different tendency of the experimental points is observed, and therefore a different slope, corresponding to the activation energy of another reaction, is observed.

In order to calculate the activation energies for the two main detected mechanisms, the following procedure was adopted. The activation energy of the first mechanism was calculated from the isoconversion plot of Fig. 9 using only the data point corresponding to high heating rate and the curves corresponding to

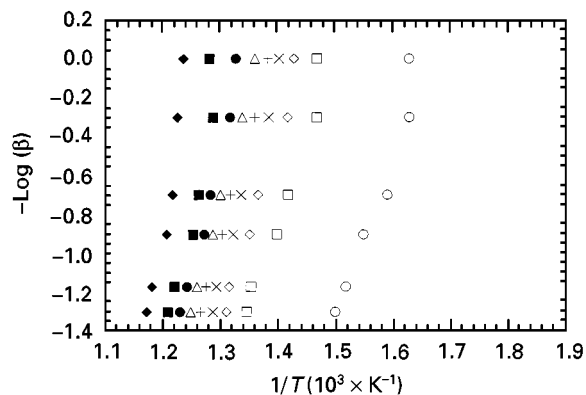


Figure 9 Flynn-Wall isoconversion plot corresponding to the maximum rate of reaction: (○) 0.10, (□) 0.20, (◇) 0.30, (×) 0.40, (+) 0.50, (△) 0.60, (●) 0.70, (■) 0.80, (◆) 0.90.

TABLE III Parameters of the kinetic model

Parameter	First mechanism	Second mechanism
n	3	2.8
$\text{Ln}K_0$ (min^{-1})	10.2	48.1
E/R (K^{-1})	8102	37149

low conversion. Another isoconversion plot was then constructed using only the data points that correspond to the conversion relative to the second mechanism (between 0.4 and 0.5); this plot is shown in Fig. 9.

These values obtained for the activation energy were then used as a starting value for the non-linear kinetic analysis. The obtained kinetic parameters are reported in Table III and the results of the kinetic model are reported in Figs 10 and 11 at different heating rates. The model gives a fair fitting of the experimental data. It must be pointed out that at higher temperature the second mechanism is the most important for the full exploitation of the ablative behaviour during the re-entry stage. Therefore, the model is useful to obtain a kinetic expression for the simulation.

4. Conclusions

Thermal analysis techniques were used to obtain the parameters of interest for an ablative system formed by a silicone resin filled with phenolic spheres, quartz spheres and fibres. The heat of ablation is calculated in a non-oxidative atmosphere while the detrimental effect of the presence of oxygen on the nature of the thermodegradation reaction is evinced by STA tests conducted in air. A general kinetic model for the degradation process was derived and their parameters computed, applying non-linear regression techniques; Combined techniques have also been used to determine a plausible mechanism in relation to the chemical composition of the polymeric matrix.

Acknowledgements

The authors acknowledge Professor L. Nicolais, Department of Material and Production Engineering,

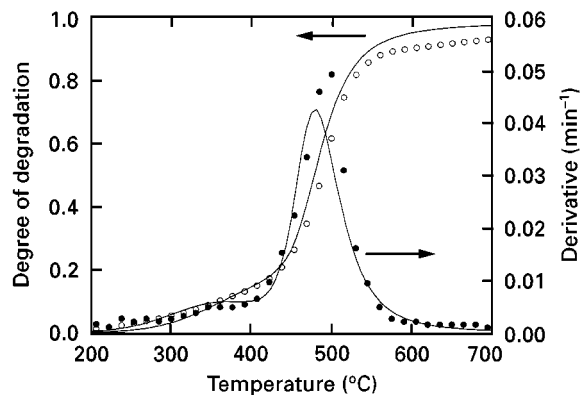


Figure 10 Comparison between the results of (—) the model and (○, ●) the experimental data for the 5°C min^{-1} run.

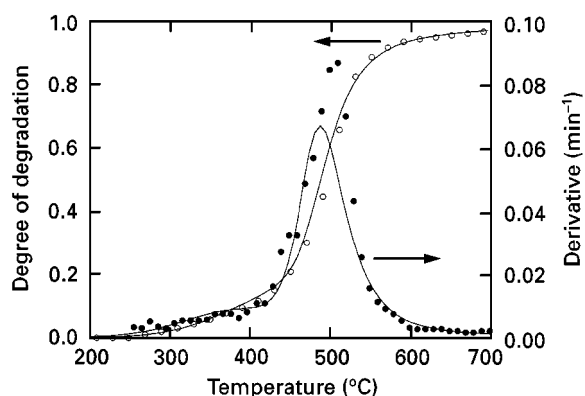


Figure 11 Comparison of the results of (—) the model and (○, ●) the experimental data for the 8°C min^{-1} run.

University of Naples, for useful advice during the research, the Alenia Spazio and Dr Josè Pace for the materials, and Dr Terzi for the help given in part of the testing.

References

1. G. F. D'ALELIO and J. A. PARKER, Eds, "Ablative Plastics" (Marcel Dekker, New York, 1971).
2. E. L. STRAUSS, in "Aspect of Polymer Degradation and Stabilization", edited by H. H. G. Jellinek, (Elsevier, New York, 1978) p. 528.
3. W. SCHNABEL, "Polymer degradation" (Hanser International, Munich, 1981).
4. T. M. McKEON, "Ablative Plastics", edited by G. F. D'Alelio and J. A. Parker, (Dekker, New York, 1971) p. 259.
5. H. E. GOLDSTEIN, *ibid.*, p. 323.
6. E. L. STRAUSS, *Chem. Eng. Prog. Sym. Ser.* **59** (1963) 232.
7. *Idem*, *J. Spacecraft* **10** (1967) 1304.
8. J. M. KENNY, A. MAFFEZZOLI, L. TORRE and G. PACE, in "39th International SAMPE Symposium" (K. Drake, J. Bauer, T. Serafini, P. Cheng (eds.) SAMPE, Los Angeles, 1994) p. 1590.
9. J. COLLINS, O. SALMASSY and L. McALISTER, in "Application of Plastic Material in Aerospace", edited by D. Simkins, (American Institute of Chemical Engineering, New York, NY, 1963) p. 9.
10. G. F. D'ALELIO, in "Ablative Plastics", edited by G. F. D'Alelio and J. A. Parker, (Marcel Dekker, New York, 1971) p. 85.
11. L. TORRE, J. M. KENNY and A. M. MAFFEZZOLI, *J. Mater. Sci.* **33** (1998) 0000.

12. H. W. LOCHTE and E. L. STRAUSS, *J. Appl. Polym. Sci.* **9** (1965) 2799.
13. O. A. HOUGEN, K. M. WATSON and R. A. RAGATZ, "Chemical Processes Principles" (Wiley, New York, 1959).
14. W. W. WENDLAND and P. K. GALLAGHER, in "Thermal Characterization of Polymeric Materials", edited by E. A. Turi, (Academic Press, New York, 1981).
15. H. L. FRIEDMAN, *Thermochim. Acta* **1** (1970) 199.
16. R. B. PRIME and J. C. SEFERIS, *J. Polym. Sci. Polym. Lett.* **24** (1986) 241.
17. K. M. NELSON, J. A. E. MANSON, J. C. SEFERIS and R. B. PRIME, *J. Appl. Polym. Sci.* **41** (1990) 301.
18. J. D. NAM and J. C. SEFERIS, *J. Polym. Sci.* **30** (1992) 455.
19. H. E. KISSINGER, *Analyt. Chem.* **29** (1957) 1709.
20. H. H. HOROWITZ and G. METZGER, *Analyt. Chem.* **35** (1963) 1464.
21. J. H. FLYNN and L. A. WALL, *Polym. Lett.* **4** (1966) 323.

*Received 10 December 1996
and accepted 18 March 1997*